Mat. Res. Bull., Vol. 28, pp. 1249-1256, 1993. Printed in the USA.
0025-5408/93 $6.00 + .00

LITHIUM EXTRACTION FROM ORTHORHOMBIC LITHIUM MANGANESE OXIDE AND THE PHASE TRANSFORMATION TO SPINEL

R J Gummow, D C Liles and M M Thackeray

Division of Materials Science and Technology, CSIR
P O Box 395, Pretoria 0001, South Africa

(September 1, 1993; Communicated by J.B. Goodenough)

ABSTRACT

Orthorhombic $LiMnO_2$ products, synthesised by the reaction of γ-MnO_2 and LiOH in argon at 600-620°C using carbon as a reducing agent, have been evaluated as electrode materials in lithium cells. Products that contained a minor proportion of a lithiated spinel phase showed greater electrochemical activity than pure $LiMnO_2$. On delithiation, $LiMnO_2$ transforms irreversibly to a spinel-type structure. A mechanism for the orthorhombic Li_xMnO_2-spinel phase transformation is proposed.

MATERIALS INDEX: lithium,manganese,oxides, spinels

Introduction

Development of rechargeable lithium batteries is limited by a concern regarding their safety. Current efforts are focused on "rocking-chair" cells which avoid the use of metallic lithium electrodes and are therefore potentially far safer than conventional lithium cells [1-3]. Carbon is the anode material of choice for "rocking-chair" cells as it gives good reversibility, high capacity and low average voltage versus lithium, resulting in high energy density cells. Carbon anodes must be coupled with lithium-rich or discharged cathodes. When the cell is first charged, lithium is transferred from the lithium-rich cathode to the carbon anode. However, not all the lithium can be recovered from the anode on the subsequent discharge; surplus cathode capacity is therefore required in the initial cathode to counteract this loss [4,5].

Lithium transition-metal oxides are being developed as cathode materials for "rocking-chair" batteries. Lithium manganese oxides, which are cheap and non-toxic, are favoured over the lithium-cobalt-oxide, $LiCoO_2$ [6], and lithium-nickel-oxide, $LiNiO_2$ [7]. There are two well-known, "lithium-rich" manganese oxides with stoichiometry $LiMnO_2$, firstly, the lithiated spinel $Li_2[Mn_2]O_4$ that has tetragonal symmetry $I4_1/amd$ (alternatively $F4_1/ddm$) [8], and secondly, orthorhombic $LiMnO_2$ with symmetry Pmmn [9]. The lithiated spinel phase has

been well characterised as a cathode for lithium batteries [10,11]. Orthorhombic $LiMnO_2$ which is conventionally synthesised at high temperature, for example, by reaction of Li_2O and Mn_2O_3 at 750°C in argon [9] does not show good electrochemical activity in lithium cells. However, a recent report by Ohzuku et al. has shown that a predominantly orthorhombic $LiMnO_2$ product, prepared by heating an equimolar mixture of γ-MnOOH and LiOH at 450°C under dry nitrogen is electrochemically active [12]; it delivers an electrode capacity of 190 mAh/g when cycled over the voltage range 2.0V - 4.25V.

The data of Ohzuku et al. have been confirmed by Reimers et al. with $LiMnO_2$ products synthesised by an ion-exchange reaction between γ-MnOOH and a 4M LiOH solution at 100°C with subsequent firing at 105°C in air, or at 200°C under argon [13]. Lithium extraction from these "low-temperature" products (referred to as LT-$LiMnO_2$) yields a disordered spinel structure. In a parallel, but independent study, we have investigated other routes to synthesise electrochemically-active orthorhombic $LiMnO_2$, the results of which are presented in this paper. We confirm the irreversible orthorhombic Li_xMnO_2-spinel phase change and propose a mechanism for the transformation.

Experimental

The synthesis of orthorhombic $LiMnO_2$ at moderate temperatures requires the use of an inert atmosphere and/or a reducing agent to prevent manganese oxidation to the tetravalent state. $LiMnO_2$ products in this study were synthesised by reaction of γ-MnO_2 (CMD) with LiOH using carbon black as a reducing agent in an argon atmosphere according to the reaction:-

$$MnO_2 + LiOH.H_2O + 0.25C \rightarrow LiMnO_2 + 0.25CO_2 + 1.5H_2O$$

An advantage of this technique is that any unreacted carbon that remains in the product may enhance the electronic conductivity of the $LiMnO_2$ electrode. Two samples were prepared, one at 620°C for 20 hours (Sample A) and one at 600°C for 4 hours (Sample B). Samples were quenched in air and stored in a desiccator.

Powder X-ray diffraction patterns were recorded using an automated Rigaku diffractometer with CuKα radiation. Galvanostatic cell-cycling data were recorded with a custom-built 16-channel cell cycler. The cathode mix consisted of $LiMnO_2$, acetylene black and ethylene propylene diene monomer (EPDM) as binder in a 84:13:3 ratio. The EPDM was dissolved in cyclohexane, mixed with $LiMnO_2$ and acetylene black and evaporated to dryness.

Cathodes were formed by pressing approximately 20 mg of cathode mix onto a stainless steel grid current collector. The anodes consisted of lithium foil pressed onto a stainless steel grid. Two-electrode, flooded, prismatic glass cells were used with a 1M solution of lithium perchlorate (Aldrich) in propylene carbonate (Aldrich 99.9%+, <50ppm H_2O) as electrolyte. Microporous polypropylene separators (Celgard 3401) were used.

Results and Discussion

The X-ray diffraction pattern of the product synthesised at 620°C (20h, Sample A) is characteristic of an essentially single-phase orthorhombic $LiMnO_2$ compound (Fig. 1a). The

product synthesised at 600°C (4h, Sample B) consisted predominantly of the orthorhombic $LiMnO_2$ phase (Fig. 1b); the X-ray diffraction pattern showed, in addition, a small peak at approximately 18° 2θ which was attributed to a minor concentration of the tetragonal, lithiated spinel phase $Li_2[Mn_2]O_4$ (Fig. 1c). Because orthorhombic $LiMnO_2$ and tetragonal $Li_2[Mn_2]O_4$ both have slightly distorted cubic-close-packed oxygen-ion arrays, it is believed that Sample B has an intergrowth structure of orthorhombic- and lithiated spinel $LiMnO_2$. The LT-$LiMnO_2$ (450°C) product reported by Ohzuku et al. also appears to contain the lithiated spinel component, but in slightly greater concentration.

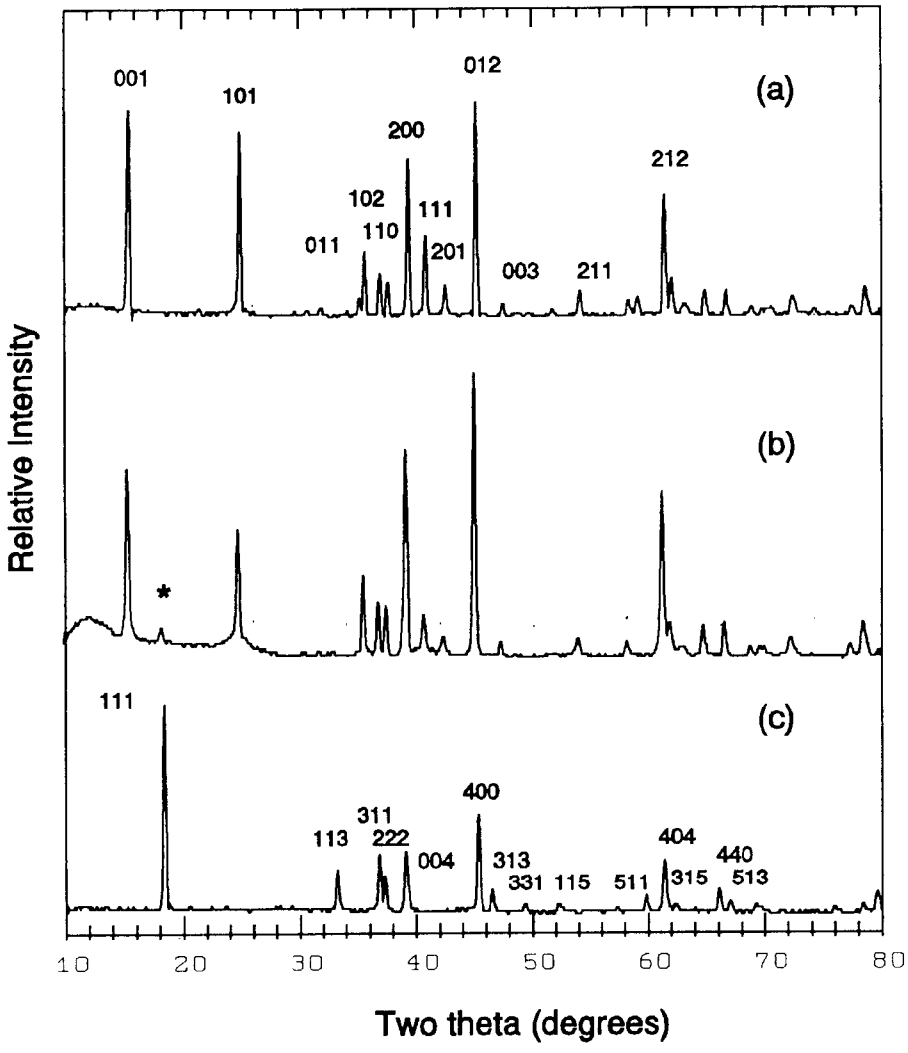

FIGURE 1

Powder X-ray diffraction patterns of:

(a) $LiMnO_2$ (Sample A) indexed to an orthorhombic unit cell (Pmmn)
(b) $LiMnO_2$ (Sample B) * = 111 peak of lithiated spinel phase
(c) $Li_2[Mn_2]O_4$ lithiated spinel indexed to a tetragonal unit cell ($F4_1/ddm$)

Fig. 2(a) shows the first, fifth and tenth charge and discharge curves of a Li/$LiMnO_2$ cell containing the single-phase $LiMnO_2$ cathode (Sample A). On the initial charge cycle, a capacity of approximately 120 mAh/g was obtained when the cell was charged to 4.45V; at

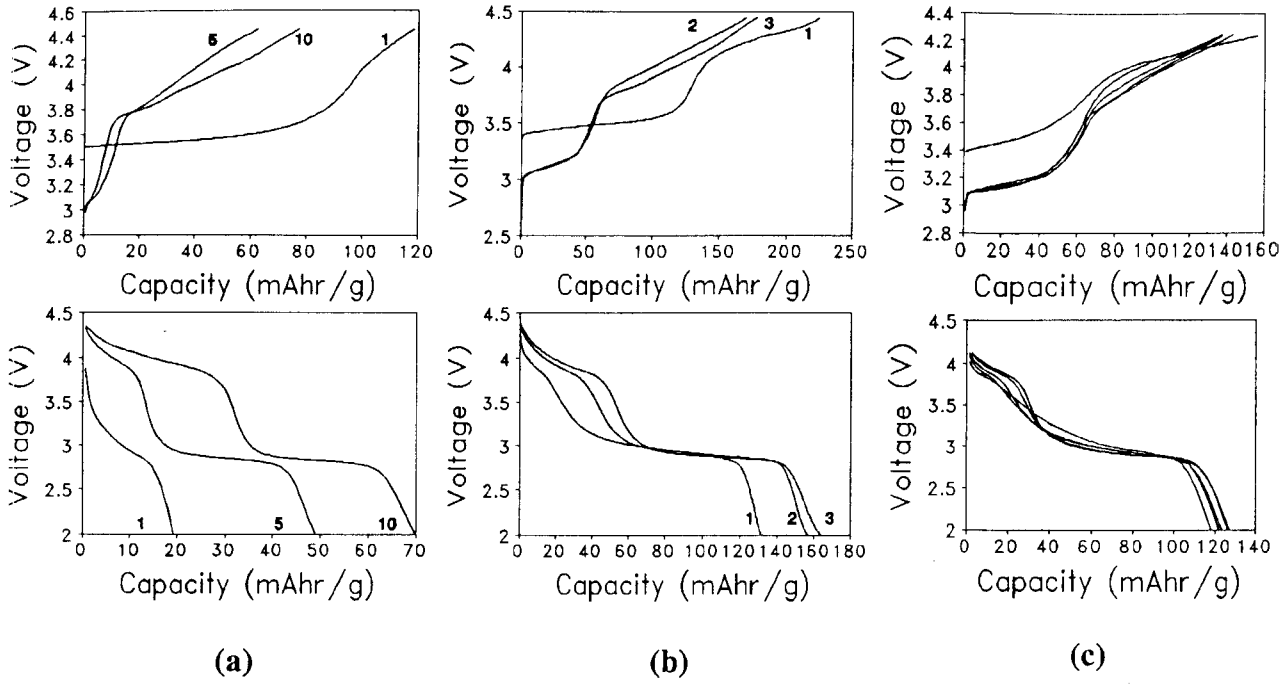

FIGURE 2

Galvanostatic cycling curves of $Li/LiMnO_2$ cells. Charge curves 0.1 mA/cm^2 and discharge curves 0.1 mA/cm^2: (a) $Li/LiMnO_2$ (Sample A) 2.50 - 4.45 V (b) $Li/LiMnO_2$ (Sample B) 2.50 - 4.45V (c) $Li/LiMnO_2$ (Sample B), cycles 1-5, 2.50 - 4.25 V.

this stage the composition of the cathode was $Li_{0.6}MnO_2$. Only $0.06Li^+$ (19mAh/g) could be reinserted on the subsequent discharge suggesting that the $LiMnO_2$ structure collapsed on lithium extraction. However, on continued cycling, the cell discharge capacity increased to reach 70mAh/g after 10 cycles. On cycling, the profile of the discharge curve became increasingly spinel-like in character with the development of two distinct reduction processes, one at 4V and the other at 3V. After ten cycles, despite the low capacity, the profile was typical of a $Li/Li_x[Mn]_2O_4$ (spinel) cell [14].

By contrast, the electrochemical activity of Sample B that contained a minor proportion of an intergrown $Li_2[Mn_2]O_4$ spinel component was significantly higher than that obtained from single-phase $LiMnO_2$, described above. After an initial charge to 4.45V to a composition $Li_{0.2}MnO_2$ the cathode delivered a discharge capacity of 130mAh/g; thereafter, the discharge capacity increased to 160mAh/g (Fig. 2(b)). When the upper voltage limit was restricted to 4.25V, a rechargeable capacity of approximately 120mAh/g was delivered by the cathode (Fig. 2(c)). The change in the voltage profile of the first and subsequent charge cycles in Figs. 2(a-c) is significant; it is indicative of an irreversible structural change that occurs during the initial extraction of lithium from the $LiMnO_2$ structure. Figs. 2(a-c) also demonstrate that in all three cells the discharge capacity delivered above 3.5V increased with cycling; this region of discharge is associated with the insertion of lithium into the tetrahedral sites of a spinel-type structure that falls within the system $Li_xMn_{2-z}O_4$ ($0 \le x \le 4/3$, $0 \le z \le 1/3$) [15]. The discharge at 3V is associated predominantly with lithium occupation of octahedral sites and the formation of a rock salt phase [8].

The phase transformation that occurs on lithium extraction was confirmed by examining the

changes in the powder X-ray diffraction patterns of several partially-charged Li_xMnO_2 cathodes ($0.2 \leq x < 1$) (Fig. 3(b-d)). The X-ray patterns clearly indicate the collapse of the parent $LiMnO_2$ structure on lithium extraction and the onset of a spinel-related phase. In $Li_{0.2}MnO_2$ (Fig. 3d), the {111},{311},{222},{400} and {440} peaks of a cubic spinel phase are clearly evident. Fig. 3e shows the X-ray diffraction pattern of a partially-discharged cathode with approximate composition $Li_{0.4}MnO_2$ obtained after 10 cycles. The shift of the spinel peaks to lower 2θ values as the lithium content is increased from $Li_{0.2}MnO_2$ (Fig. 3d) to $Li_{0.4}MnO_2$ (Fig. 3e) indicates an expansion of the oxygen-ion array. The X-ray diffraction pattern of the spinel phase in Fig. 3e could be indexed to a cubic unit cell with $a = 8.260(2)$Å. Surprisingly, the lattice constant is slightly larger than that expected for a spinel structure of nominal composition $Li_{0.8}[Mn_2]O_4$ ($a = 8.181(1)$Å) which was determined from a plot of a versus x in $Li_{1-x}[Mn_2]O_4$ [16].

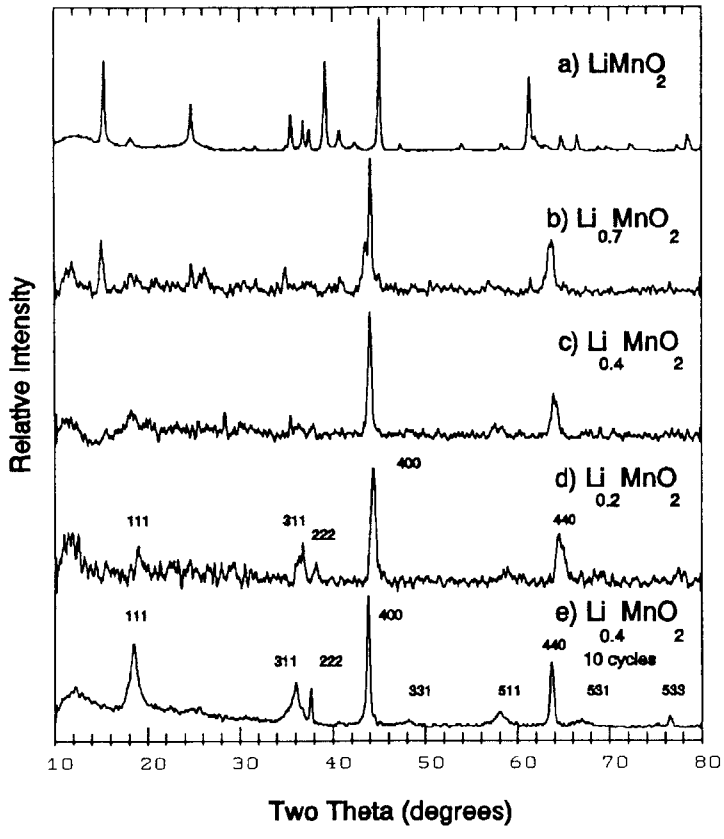

FIGURE 3

Powder X-ray diffraction patterns of Li_xMnO_2 (Sample B)

(a) $x = 1.0$ (b) $x = 0.7$ (c) $x = 0.4$
(d) $x = 0.2$ (e) $x \approx 0.4$ after 10 cycles.

The maximum discharge capacity obtained from Li_xMnO_2 electrodes in this investigation (160mAh/g) is inferior to the capacity of LT-$LiMnO_2$ (190 mAh/g) synthesized at 450°C [12]. This can be attributed to the higher synthesis temperature (600°C) used in our preparation of the electrodes. It is worthwhile to note, however, that the discharge profiles of our Li/HT-$LiMnO_2$ cells resemble more closely the discharge profiles of Li/HT-$Li_x[Mn_2]O_4$ (spinel) cells with distinct 4V and 3V regions, whereas Li/LT-$LiMnO_2$ cells discharge most of their capacity at approximately 3V; the latter type of discharge is

characteristic of lithium cells with "low-temperature" spinel cathodes such as $LiMn_2O_{4+\delta}$ ($0 < \delta \leq 0.5$) which are synthesised typically at 350°C-420°C [15,17].

The orthorhombic $LiMnO_2$ to spinel transformation.

The orthorhombic $LiMnO_2$ phase has a rock salt structure with a distorted cubic-close-packed oxygen anion array in which zig-zag layers of lithium and manganese cations alternate with one another as depicted in Fig. 4a. Although the structure can be described as layered, it differs from the well-known layered $LiCoO_2$ and $LiNiO_2$ structures in which alternate layers of lithium and cobalt (nickel) cations lie parallel to the layers of close-packed oxygens ions (Fig. 4b). The structure of the lithiated spinel phase $Li_2[Mn_2]O_4$ (which also has the rock salt stoichiometry $LiMnO_2$) is illustrated in Fig. 4c. In this structure the manganese ions are distributed between the close-packed oxygen planes in a 3:1 ratio; the $[B_2]O_4$ framework (B=metal cation) of an $Li[B_2]O_4$ spinel which contains a three-dimensional network of interconnected interstitial sites for lithium ion diffusion is depicted in Fig. 4d; it provides a remarkably stable host framework structure for lithium insertion/extraction reactions.

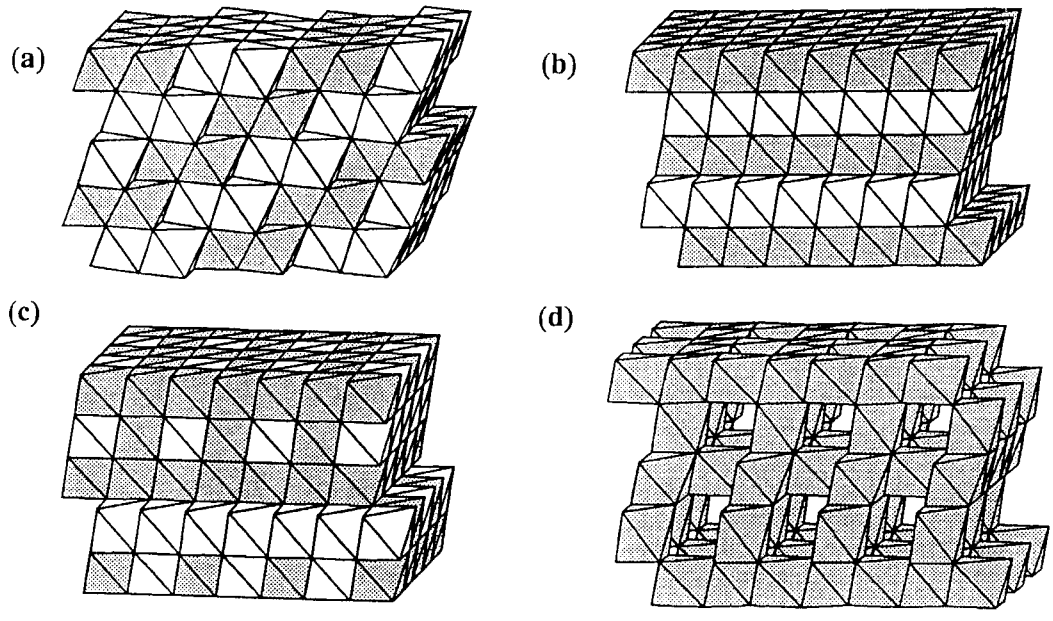

FIGURE 4

Schematic diagrams of the structures of:
(a) orthorhombic $LiMnO_2$ (b) layered $LiMO_2$ (M=Co,Ni)
(c) lithiated spinel $Li_2[Mn_2]O_4$, and (d) the $[B_2]O_4$ spinel framework.
Shaded octahedra are occupied by transition-metal cations and clear octahedra are occupied by lithium.

Lithium extraction from the orthorhombic $LiMnO_2$ structure necessitates the migration of lithium cations from their octahedral positions, via adjacent face-shared tetrahedra, to neighbouring octahedral sites previously occupied by lithium. In orthorhombic $LiMnO_2$, each tetrahedron shares faces with at least one occupied manganese octahedron; this situation is similar to that found in the layered $LiMO_2$ oxides (M=Co,Ni) in which lithium diffusion is known to be rapid [18,19]. In Li_xCoO_2 and Li_xNiO_2, the layered MO_2 subarray

remains intact, at least for $0.5<x\leq1$; lithium extraction is accompanied by an expansion of the *c* axis and an increase in the *c/a* ratio. By contrast, a delithiated orthorhombic $LiMnO_2$ structure is unstable; lithium extraction from the zig-zag layers is accompanied by a migration of manganese cations into some of the octahedral sites left vacant by the extracted lithium to yield a stable spinel-type structure.

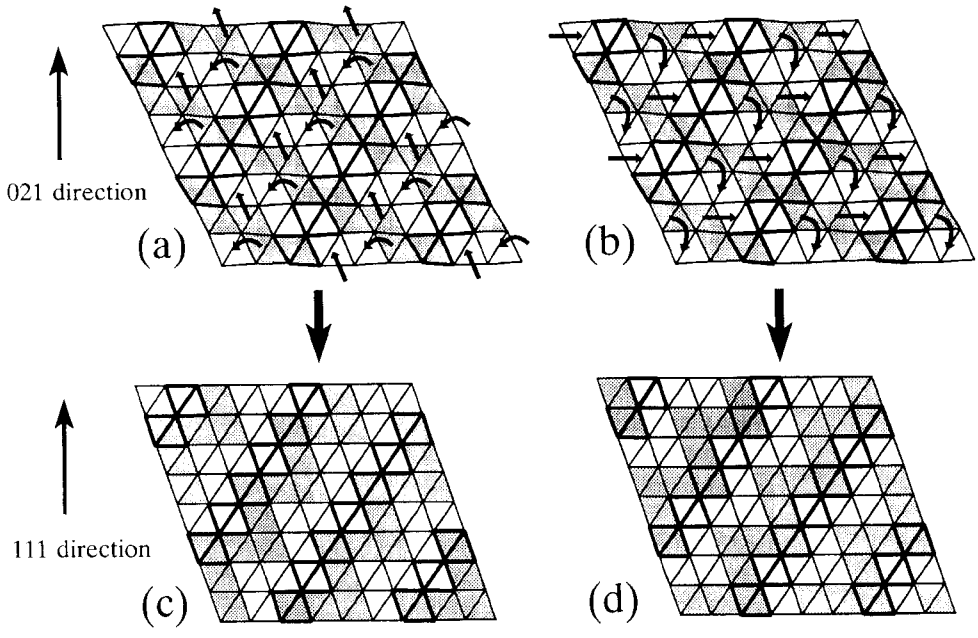

FIGURE 5
Schematic diagram of the transformation from the orthorhombic to the spinel structure in Li_xMnO_2.

A possible mechanism for the structural transformation of the MnO_2 framework in orthorhombic $LiMnO_2$ to the ideal $[Mn_2]O_4$ spinel framework on lithium extraction from $LiMnO_2$ is given in Fig. 5(a-d). Two parallel slices that alternate through the orthorhombic Li_xMnO_2 structure are shown in Fig. 5(a and b); the corresponding slices of the spinel structure are given in Fig. 5(c and d), respectively. The shaded octahedra are occupied by manganese cations whereas the clear octahedra represent either lithium-occupied or vacant octahedra.

It is evident that certain discrete planes consisting of alternating strings of fully-occupied Mn and Li (or vacant) octahedra in the parent orthorhombic $LiMnO_2$ structure and in the spinel product are unaffected by the transformation; these planes are highlighted in bold outline in Fig. 5(a-d); the transformation takes place in the oxygen framework between these planes. Lithium extraction from the zig-zag channels causes a displacement of 50% of the manganese ions into neighbouring octahedra left vacant by the extracted lithium ions as indicated by the arrows in Fig. 5(a and b). In the ideal transformation process, the displacement of one manganese ion from its octahedral position through a face-shared tetrahedron (curved arrow) into a vacant octahedral site causes the cooperative displacement of one other manganese ion (straight arrow). The direction of the manganese-ion pair displacements in Fig. 5a is opposite to that in the next slice (Fig. 5b). These displacements generate the 3:1 spinel ratio of manganese ions in alternate layers between the close-packed oxygen planes (Fig. 5(c and d)). In practice, the electrochemical and X-ray diffraction data show that a few cycles are necessary to accomplish the transformation and

that metastable and disordered spinel-type structures are produced as intermediate phases.

Conclusions

Orthorhombic $LiMnO_2$ products synthesised at 600°C have been evaluated as cathode materials in lithium cells. The $LiMnO_2$ structure is destabilised by lithium extraction and transforms on cycling to a spinel-type phase. The presence of a small amount of intergrown lithiated spinel in the initial $LiMnO_2$ cathode appears to facilitate the transformation and to improve the electrochemical performance when compared to $LiMnO_2$ cathodes that are initially single-phase. $LiMnO_2$ electrodes when synthesised by this method yield a rechargeable capacity of 160 mAh/g when cycled between 4.45V and 2.0V; this is slightly inferior to the capacities that can be achieved from $LiMnO_2$ electrodes synthesised at lower temperature (190 mAh/g). The data emphasise the stability of the $[B_2]O_4$ framework of $Li[B_2]O_4$ spinels and its utility as an insertion electrode for rechargeable lithium cells.

References

1. J M Tarascon and D Guyomard, *J. Electrochem. Soc.*, **139**, 937 (1992).
2. J R Dahn, U von Sacken, M W Juzkow and H Al-Janaby, *J. Electrochem. Soc.*, **138**, 2207 (1991).
3. T Nagaura and K Tozawa, *Prog. Batt. and Solar Cells*, **9**, 209 (1990).
4. Z X Shu, R S McMillan and J J Murray, *J. Electrochem. Soc.*, **140**, 922 (1993).
5. R Fong, U von Sacken and J R Dahn, *J. Electrochem. Soc.*, **137**, 2009 (1990).
6. W D Johnston, R R Heikes and D Sestrich, *J. Phys. Chem. Solids*, **7**, 1 (1958).
7. J B Goodenough, D G Wickham and W J Croft, *J. Appl. Phys.*, **29**, 382 (1958).
8. M M Thackeray, W I F David, P G Bruce and J B Goodenough, *Mat. Res. Bull.*, **18**, 461 (1983).
9. G Dittrich and R Hoppe, *Zeit fur Anorg Allg Chemie*, **368**, 262 (1969).
10. J M Tarascon and D Guyomard, *J. Electrochem. Soc.*, **138**, 2864 (1991).
11. J M Tarascon, D Guyomard and G L Baker, *J. Electrochem. Soc.*, (1993). In press.
12. T Ohsuku, A Ueda and T Hirai, *Chem. Express*, **7**, 193 (1992).
13. J N Reimers, C W Fuller, E Rossen and J R Dahn, *J. Electrochem. Soc.*, (1993). Submitted for publication.
14. J M Tarascon, C Wang, F K Shokoohi, W McKinnon and S Colson, *J. Electrochem. Soc.*, **138**, 2859 (1991).
15. M M Thackeray, A de Kock, M H Rossouw, D Liles, R Bittihn and D Hoge, *J. Electrochem. Soc.*, **139**, 363 (1992).
16. W I F David, M M Thackeray, L A de Picciotto and J B Goodenough, *J. Solid State Chem.*, **67**, 316 (1987).
17. A de Kock, M H Rossouw, L A de Picciotto, M M Thackeray, W I F David and R M Ibberson, *Mat. Res. Bull.*, **25**, 657 (1990).
18. M G S R Thomas, P G Bruce and J B Goodenough, *Solid State Ionics*, **57**, 17, 13 (1985).
19. P G Bruce, A Lisowska-Oleksiak, M Y Saidi and C A Vincent, *Solid State Ionics*, **57**, 353 (1992).